An experimental study on model continuous beam bridge with steel deck

Autor(en): **Naruoka, Masao / Okabe, Toshimasa / Hori, Koichi**

Objekttyp: **Article**

Zeitschrift: **IABSE publications = Mémoires AIPC = IVBH Abhandlungen**

Band (Jahr): **18 (1958)**

PDF erstellt am: **27.05.2024**

Persistenter Link: https://doi.org/10.5169/seals-16511

An Experimental Study on Model Continuous Beam Bridge with Steel Deck

Recherches sur modèle concernant un pont à poutre continue avec tablier métallique

Modelluntersuchung einer Durchlaufträgerbrücke mit Stahlfahrbahn

MASAO NARUOKA, Professor of Kyoto University, Kyoto, Japan
TOSHIMASA OKABE and KOICHI HORI, Hull Designing Section, Ship Designing Department, Nagasaki Works, Mitsubishi Shipbuilding and Engineering Co., Ltd., Japan

1. Introduction

In the design of the Köln-Mülheim suspension bridge, the steel deck (steel plate stiffened transversely and longitudinally) was used instead of a reinforced concrete slab and also as the upper flange of stiffened girders, and thus a considerable reduction in the steel weight was possible. Thereafter the steel deck was used in the design of many box girder bridges such as Düsseldorf-Neuss Bridge, Bürgermeister-Schmidt Bridge and Porta Bridge and also of plate girder bridges such as Kurpfalz Bridge and St.-Alban Bridge.

In the design of the Kurpfalz Bridge, the steel deck was calculated by the theory of orthogonally anisotropic (orthotropic) plates and moreover, the load distribution coefficient of each girder was calculated by the theory of the orthotropic plate assuming the center span part as the orthotropic plate having the reduced flexural rigidity in the bridge axis which is simply supported on the two opposite edges (piers) and supported by flexural beams on the other two opposite edges. This is the conventional method but much remains to be solved.

From this point of view, the authors tried to make an experimental study on the model continuous girder bridge with steel deck and to contribute something to the design of the bridge of this type.

2. Details of Model Continuous Girder Bridge

The model is a three span continuous girder bridge with steel deck, and the details are as follows.

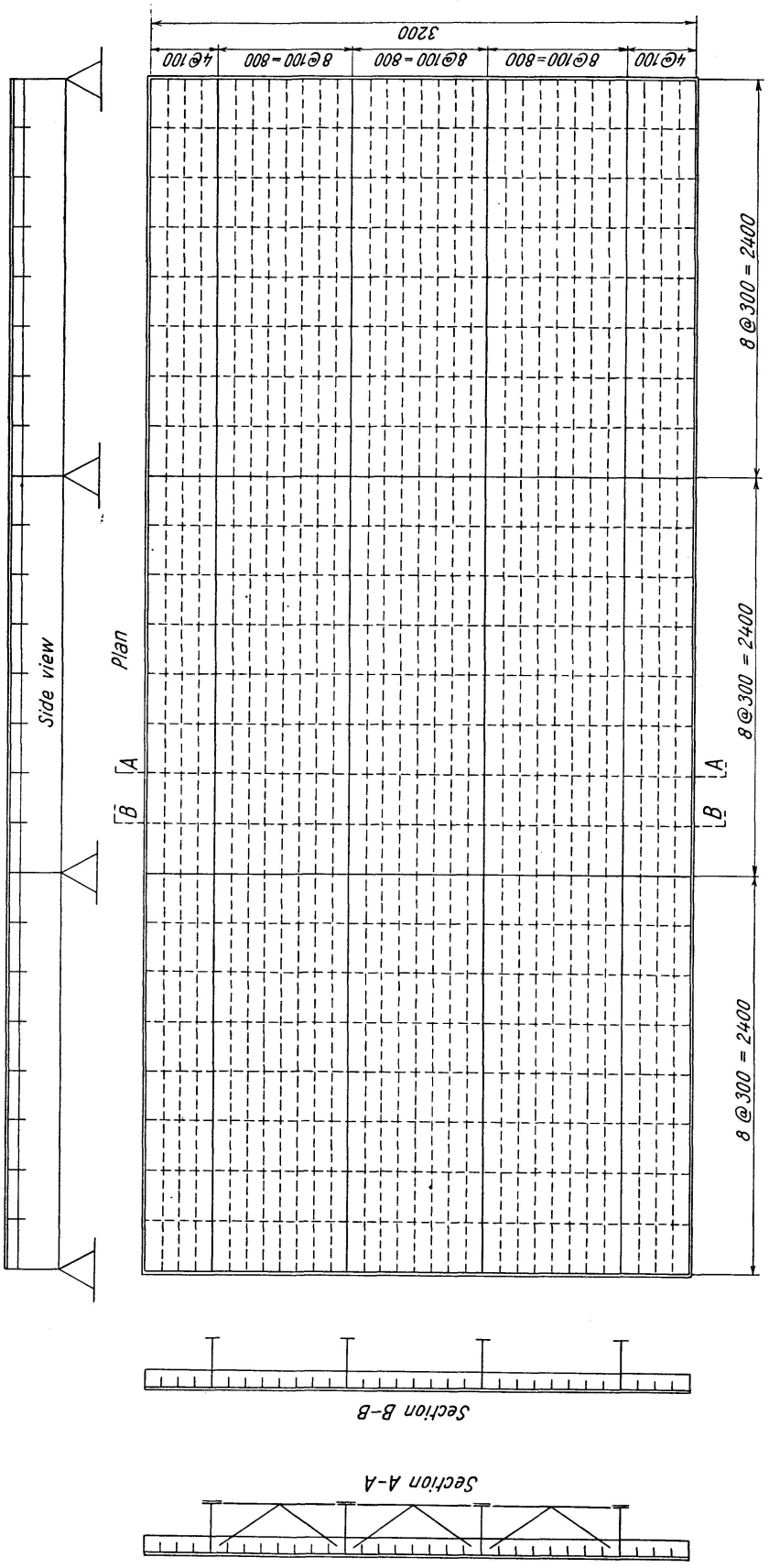
3200
4@100
8@100=800
8@100=800
8@100=800
4@100
8@300=2400
8@300=2400
8@300=2400
Side view
Plan
A
B
A
B
Section B-B
Section A-A

Fig. 1.

a)	Length and span	3 @ 2.400 = 7.200 m.
b)	Width	0.400 + 3 @ 0.800 + 0.400 = 3.200 m.
c)	Main girder	4, spaced at equal distances of 80 cm web plate: 6×300, lower flange: 12×120.
d)	Steel deck	deck plate: 6 mm thick; longitudinal stiffener: 6×50, spaced at equal distances of 10 cm; transverse stiffener: plate 12×100 spaced at equal distances of 30 cm.
e)	Sway bracing	angle $40 \times 40 \times 5$ located at equal distances of 60 cm.

The plan, side view and cross sections of the model are shown in fig. 1. This is only a model bridge and is not of the reduced dimensions of the existing bridge on account of the loading device, transportation and welding deformation. That is, the bridge width and depth are large compared with the span, and also the web plate is thick in comparison with the actual thickness of existing bridges.

3. Loading Device and Measurement

The load was applied by hydraulic jacks, the magnitude of the hydraulic pressure was decided by a pressure gage and load cell which was located between the jacks and model.

The strain was picked up by an electrical resistance wire strain gage with bakelite base and measured by a strain indicator. The deflection was observed by a dial gage.

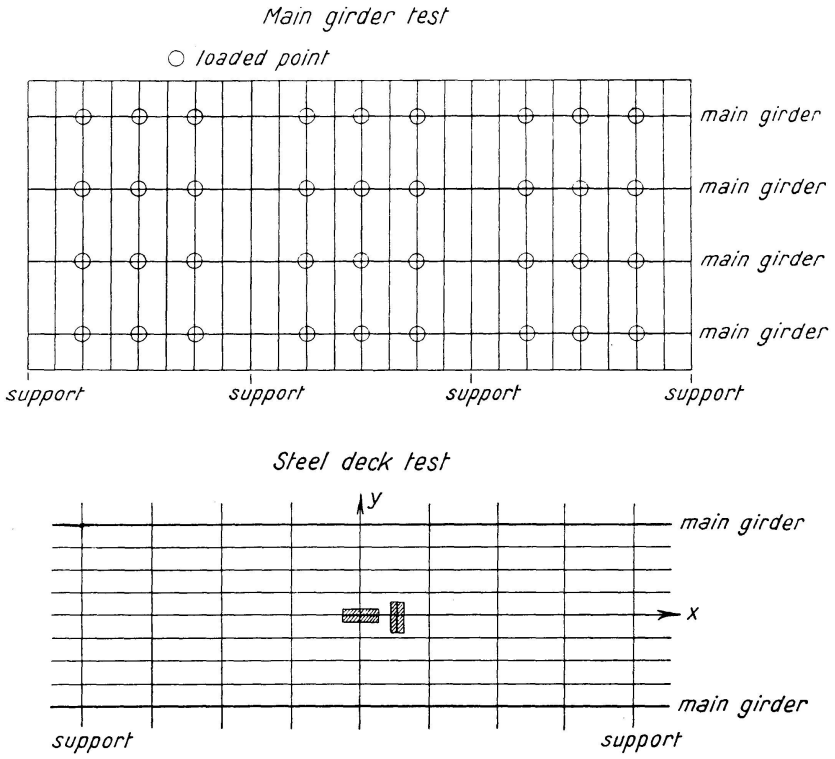

Fig. 2.

The load was applied to various points shown in fig. 2 and at each step of loading the strain and deflection were measured. Thus, the load distribution in the transverse direction was obtained and the observed results were compared for the two cases of the bridges with and without sway bracings. And also the influence lines of the bending moment at midspan and support were observed.

The stress of the steel deck is very complicated. In order to research this stress, the stress on the upper surface of the steel grid floor was measured.

4. Method of Analysis

In order to analyse the girder structure of this type, the following methods can be considered.

1. Method of analysing the structure as a grillage girder bridge such as F. Leonhardt's method and H. Homberg's method.

2. Method of analysing the structure as a parallel girder bridge with uniformly distributed cross girder such as H. Homberg's method, A. J. S. Pippard's method and Winowsky-Krieger's method.

3. Method of analysing the structure as a three span continuous orthotropic plate with two opposite free edges.

Table 1. Fundamental Data of Model Beam Bridge

a) Moment of inertia of main girder		
load	skew-symmetrical load on inner girders	the other
girder	inner girder	
effective width	$2\lambda/3 = 53.4$ cm	$\lambda = 80$ cm
moment of inertia	12,000 cm^4	13,560 cm^4
	containing the upper flange and longitudinal stiffeners	

b) Converted moment of inertia of main girder		
Effective width	for side span	for center span
$\lambda = 80$ cm	11,860 cm^4	13,920 cm^4
$2\lambda/3 = 53{,}4$ cm	10,980 cm^4	12,960 cm^4

c) Converted moment of inertia of transverse stiffener				
	single load	symmetrical load	skew-symmetrical load	effective width
with sway bracing	2,270 cm^4	2,370 cm^4	1,350 cm^4	60 cm
without sway bracing		302 cm^4		30 cm

Pippard's and Krieger's methods were proposed for the simply supported girder bridge and can not be applied to the continuous girder structure. The authors' method may be classified into type (2) and can be applied to the continuous structure. The detail of the solution is described in Appendix B.

The experimental values were compared with the theoretical values which were calculated by various methods. In the analysis of this girder bridge structure, much attention must be paid to the effect due to shearing force, because the depth of this girder is larger than that of the general girder bridges. Authors' method of analysis considers the effect due to shearing force.

The fundamental data for the calculation are shown in table 1.

The method of calculation for the reduced moment of inertia of the cross girder is shown in Appendix A.

5. Experimental Results on Main Girder

1. Deflection. The deflection measured at the mid-span of each girder of the loaded span is shown in table 2, compared with the theoretical values calculated by the authors' method, and also the measured load distribution coefficient is shown in table 3 with the theoretical coefficient.

2. Stress of lower flange. The stresses of the lower flange measured at the mid-span of each girder of the loaded span under mid-span loading are shown in table 4, compared with the theoretical values calculated by the authors' analytical method, F. Leonhardt's method and the theory of the orthotropic plate.

Table 2. Measured Deflection (mm) at the Mid-Span Section of Each Girder Under the Mid-Span Loading of 30 t (fig. 3)

load	girder	with sway-bracing				without sway-bracing			
		a	b	c	d	a	b	c	d
1.	Experimental value	3.140	0.738	−0.010	−0.213	3.333	0.490	−0.098	−0.050
	Authors' value	3.222	0.752	−0.191	−0.252	3.220	0.570	−0.180	−0.070
2.	Experimental value	0.738	2.060	0.708	−0.020	0.515	2.545	0.650	−0.110
	Authors' value	0.725	1.956	1.014	−0.164	0.580	2.220	0.910	−0.190
3.	Experimental value	2.720	0.580	−0.025	−0.135	2.905	0.510	−0.050	−0.020
	Authors' value	2.754	0.602	−0.171	−0.200	3.194	0.587	−0.164	−0.086
4.	Experimental value	0.640	1.970	0.685	−0.010	0.420	2.295	0.565	−0.045
	Authors' value	0.579	1.717	0.838	−0.149	0.601	2.197	0.911	−0.179
2′.	Experimental value	0.76	2.60	2.69	0.76	0.51	3.00	3.08	0.47
	Authors' value	0.56	2.97	2.97	0.56	0.39	3.13	3.13	0.39
4′.	Experimental value	0.63	2.53	2.53	0.67	0.49	3.04	3.09	0.52
	Authors' value	0.43	2.56	2.56	0.43	0.42	3.11	3.11	0.42

Table 3. Comparison of Load Distribution Coefficients (fig. 3)

load	Method of Analysis	with sway-bracing				with sway-bracing				without sway-bracing			
		a	b	c	d	a	b	c	d	a	b	c	d
1	L.	89.1	17.5	−2.5	−4.2	88.5	19.3	−4.2	−3.7	96.6	7.1	−3.9	−0.2
	G-M.	84.4	23.1	−1.9	−5.6	83.4	23.8	−2.6	−4.6	90.5	14.4	−4.4	−0.5
	A.	91.6	15.1	−5.4	−1.3					95.6	10.2	−7.1	−1.3
	E.	85.2	16.7	0.0	−1.9	85.2	16.7	0.0	−1.9	92.5	10.2	−3.5	−1.9
2	L.	18.0	61.2	23.6	−2.8	19.3	57.3	27.7	−4.2	7.1	82.0	14.8	−3.9
	G-M.	21.4	57.3	21.9	−0.1	22.7	52.7	26.6	−2.0	14.3	71.6	18.6	−4.5
	A.	15.6	62.6	27.7	−6.0					10.9	80.1	16.9	−7.9
	E.	15.6	67.8	18.7	−2.1	15.6	67.8	18.7	−2.1	8.3	83.4	12.5	−4.2
3	L.	90.1	16.3	−2.8	−3.5	89.5	18.0	−4.6	−3.0	96.9	6.3	−3.5	0.2
	G-M.	84.8	22.1	−1.3	−5.6	83.9	23.5	−2.8	−4.6	90.9	13.5		
	A.	90.6	15.9	−3.5	−3.1					95.1	10.2	−5.7	0.4
	E.	87.2	16.0	1.0	−4.5	87.2	16.0	1.0	−4.5	93.6	9.5	−2.1	−1.0
4	L.	16.6	63.8	22.8	−3.1	18.7	59.4	27.2	−4.6	6.3	83.8	13.4	−3.5
	G-M.	20.5	60.4	20.2	−1.1	21.8	54.2	26.4	−2.4	12.7	74.8	17.1	−4.6
	A.	16.5	63.0	24.6	−4.1					11.0	81.3	14.2	−6.6
	E.	16.7	66.7	16.7	0.0	16.7	66.7	16.7	0.0	9.0	79.5	13.6	−2.1
Remarks		$I = 2370\ cm^4$ for symmetrical loading $I = 1350\ cm^4$ for skew-symmetrical loading were used				$I = 2370\ cm^4$ was used							

L. = F. Leonhardt's method, G-M. = theory of orthotropic plate, A. = Authors' method, E. = Experimental value. These notations are the same as in tables 4∼6.

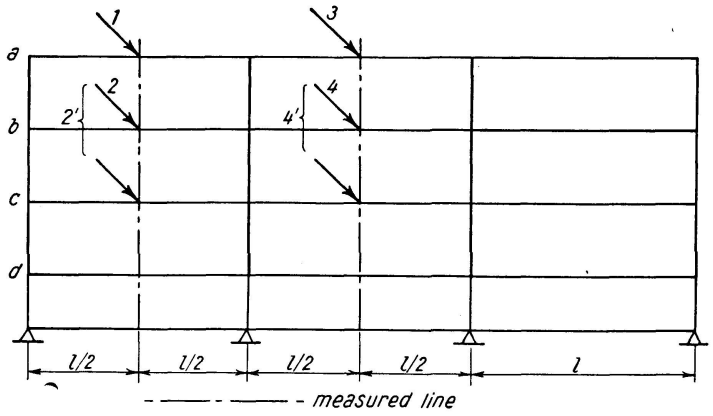

Fig. 3.

Table 4. Stresses of Lower Flange (kg/cm²) Measured at the Mid-Span of Each Girder Under Mid-Span Loading of 30 t (fig. 3)

load	Method of Analysis	with sway-bracing				without sway bracing			
		a	b	c	d	a	b	c	d
1	E.	2385	480	− 48	−120	2543	248	− 63	− 15
	A.	2350	390	−140	− 34	2442	263	−184	− 35
	L.	2335	459	− 65	−110	2535	186	−103	− 5
	G-M.	2210	605	− 50	−147	2370	377	−115	− 13
2	E.	397	1665	410	− 38	268	2070	403	− 63
	A.	400	1620	720	−153	281	1803	691	−202
	L.	472	1603	619	− 73	186	2150	388	−103
	G-M.	561	1560	574	− 26	377	1875	487	−118
3	E.	2068	425	− 55	− 80	2170	230	− 45	− 10
	A.	1977	348	− 76	− 67	2078	223	−125	− 9
	L.	2050	369	− 63	− 79	2190	142	− 79	− 4
	G-M.	1915	500	− 30	−126	2050	305	−100	0
4	E.	373	1475	375	− 50	205	1890	305	− 70
	A.	360	1380	540	− 89	241	1563	530	−144
	L.	375	1440	515	− 70	142	1892	303	− 79
	G-M.	464	1365	456	− 26	287	1690	386	−104
2′	E.	395	2020	2180	400	110	2290	2415	190
	A.	250	2320	2320	250	80	2495	2495	80
	L.	400	2220	2220	400	83	2540	2540	83
	G-M.	535	2074	2074	535	260	2360	2360	260
4′	E.	212	1690	2150	320	100	1900	2000	110
	A.	270	1920	1920	270	97	2095	2095	97
	L.	300	1955	1955	300	65	2195	2195	65
	G-M.	240	1820	1820	240	185	2075	2075	185

Next, the stresses measured at the mid-span of each girder of the span loaded at $\frac{l}{4}$ and $\frac{3l}{4}$ section are shown in table 5 and the distribution coefficients are shown in table 6.

The authors' values were obtained by superposing the results calculated by the reduced moment of inertia for the symmetrical and skew-symmetrical cases shown in fig. 16. The load distribution coefficients calculated by this method are shown in the left column of table 3. The values calculated by the reduced moment of inertia of the sway bracing for the single loading are shown at the same time in the center column of table 3. The reduced moments of inertia for cases b) and c) of fig. 16 are almost equal and the value for case b) is used, for single loading.

Table 5. Stresses at the Lower Flange (kg/cm²) Measured at the Mid-Span of Each Girder Under $\frac{l}{4}$ and $\frac{3l}{4}$ Loading of 30 t (fig. 4)

load	Method of Analysis	a	b	c	d	load	Method of Analysis	a	b	c	d
5	E.	973	345	− 8	−68	8	E.	250	413	263	−10
	A.	1045	310	−63	−61		A.	220	515	361	−69
	L.	1065	210	−30	−50		L.	188	639	246	−29
6	E.	273	448	268	−10	9	E.	760	270	−18	−55
	A.	310	547	440	−63		A.	741	225	−49	−43
	L.	215	734	282	−33		L.	940	183	−26	−44
7	E.	925	305	30	−65	10	E.	240	350	238	−10
	A.	909	220	−69	−28		A.	225	376	323	−49
	L.	940	183	−26	−44		L.	214	723	279	−33

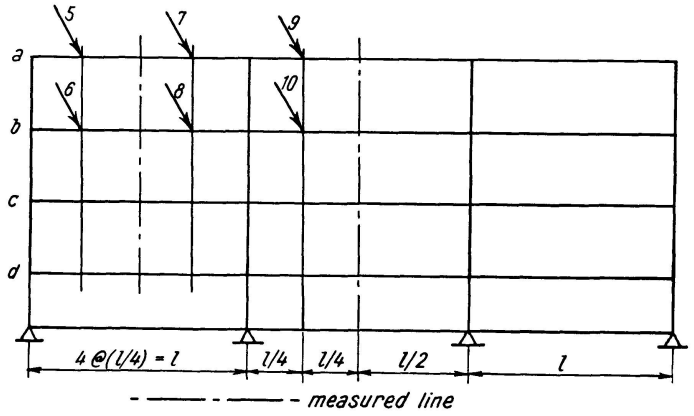

Fig. 4.

Table 6. Load Distribution Coefficients at the Mid-Span Section Under the $\frac{l}{4}$ and $\frac{3l}{4}$ Loading (fig. 4)

load	Method of Analysis	a	b	c	d	load	Method of Analysis	a	b	c	d
5	A.	85	25	−5	−5	8	A.	25	44	36	−5
	E.	78	27	1	−6		E.	26	43	29	−1
6	A.	25	44	36	−5	9	A.	85	26	−6	−5
	E.	28	45	27	0		E.	77	27	2	−6
7	A.	85	25	−5	−5	10	A.	26	43	37	−5
	E.	77	27	2	−6		E.	29	42	29	0

The comparison of the stress of the lower flange of the main girder of the bridges with and without sway bracings is shown in table 7.

3. Influence line of bending moment. The influence lines of bending moments at mid-span and supports experimentally obtained for only the girders concerned are shown in fig. 5. In the calculation of the bending moment from the measured stress, the effective width of the upper flange of the main girder was assumed as 100% and 50% of the girder spacing for the mid-span and support respectively.

4. Stress of sway bracing. The stresses of the sway bracing at the mid-span of the side and center span under the mid-span loading are shown in table 8.

The theoretical values were obtained by the method proposed by F. Leonhardt, that is, under the assumption of the sway bracing being at the mid-span, the flexural rigidity of which is 1.6 times larger than that of the individual one.

Table 7. Influence of Sway-Bracing upon the Stresses at the Lower Flange of Mid-Span Section and Load Distribution Coefficients (fig. 3)

load	girder	stress (kg/cm²)		load distribution coef. (%)	
		with	without	with	without
		sway-bracing		sway-bracing	
1	a	2385	2545	88.4	93.7
	b	480	248	17.8	9.1
	c	−48	−63	−1.8	2.3
	d	−120	−15	−4.4	−0.5
2	a	397	268	16.4	10.0
	b	1665	2070	68.5	77.3
	c	410	403	16.8	15.1
	d	−38	−63	−1.6	−2.4
3	a	2068	2170	87.8	92.6
	b	425	230	18.0	9.8
	c	−55	−45	−2.3	−1.9
	d	−80	−10	−3.4	−0.4
4	a	373	205	17.1	8.8
	b	1475	1890	68.0	81.1
	c	375	305	17.2	13.1
	d	−50	−70	−2.3	−3.0

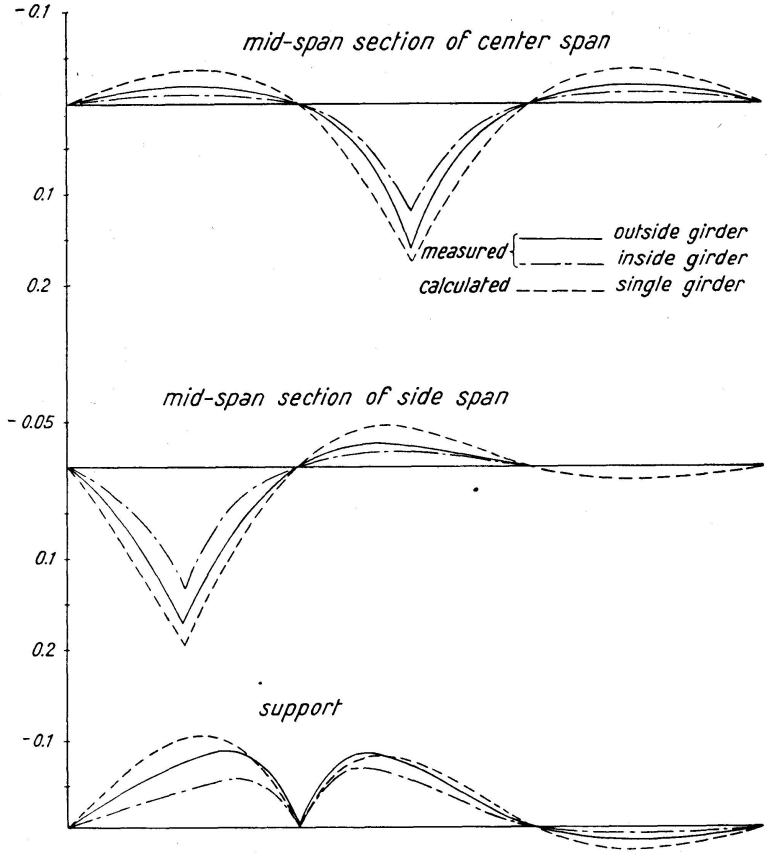

Fig. 5. Influence Line of Bending Moment. Unit: l.

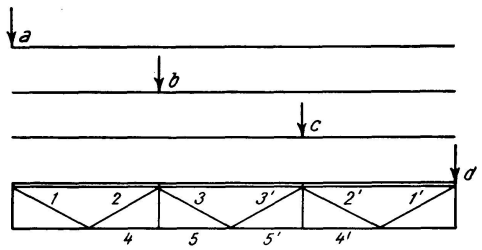

Fig. 6.

6. Discussion on the Experimental Results of Main Girder

1. For the deflection and the stress of the lower flange of the main girder and the stress of the sway bracing, the measured and theoretical values are almost equal and show good agreement.

2. The sway bracing has no purpose of distributing the applied load to each girder, but its influence on the load distribution can be clearly understood. The sway bracing has been designed customally without calculation, but because a considerable amount of stress exists, the sway bracing must be designed for the single concentrated load.

3. The theoretical values for the single loading on the main girder with the sway bracing were obtained by superposing the results of the two cases of the

Table 8. Stresses of the Sway Bracing of the Mid-Span Section Measured Directly Under the Mid-Span Loading of 30 t (fig. 6)

	load	a		b		c		d	
		exp.	theo.	exp.	theo.	exp.	theo.	exp.	rheo.
center span	1	−770	− 570	1080	870	0	0	−280	− 290
	2	710	570	−1250	−870	0	0	240	290
	3	250	270	−1030	−870	1210	870	−350	− 270
	3′	−310	− 280	1160	870	−1040	−870	340	280
	2′	360	290	50	0	−1040	−870	770	570
	1′	−360	− 290	− 40	0	1020	870	−760	− 570
	4	−780	− 825	1580	1410	− 50	0	−340	− 470
	5	−940	− 825	1160	1410	− 180	0	−540	− 470
	5′	−360	− 470	− 100	0	1330	1410	−850	− 825
	4′	−590	− 470	− 80	0	1440	1410	−710	− 825
side span	1	−580	− 625	1200	940	− 24	− 35	−330	− 340
	2	660	625	−1000	−940	0	35	290	340
	3	160	290	−1140	−970	1080	970	−420	− 290
	3′	−350	− 290	1220	970	− 960	−970	290	290
	2′	290	340	0	35	−1040	−970	700	625
	1′	−260	− 340	− 40	− 35	1090	970	−780	− 625
	4	−700	−1000	1260	1560	− 80	− 35	−420	− 540
	5	−910	−1000	1260	1560	100	− 35	−600	− 540
	5′	−590	− 540	150	− 35	1210	1560	−970	−1000
	4′	−360	− 540	− 35	− 35	1410	1560	−890	−1000

symmetrical and skew-symmetrical loadings as described above. On the other hand, if we calculate, using the reduced moment of inertia of the sway bracing for the single load or symmetrical load, without performing the superposition described above, no great difference is recognized for the outside main girder, but a considerable difference between the measured and theoretical values can be noticed for the inside main girder.

4. The various methods of analysis give almost the same values for the deflection and stress at mid-span, but the value of the load distribution under the special loading at $l/4$ and $3l/4$ differs considerably from the value obtained for the mid-span loading. This fact can not be explained by F. Leonhardt's method or the theory of the orthotropic plate, but is explainable only by the authors' analytical method and H. Homberg's method.

5. The form of the influence line of the bending moment at the mid-span of the side and center spans does not differ considerably from that of the single continuous beam. Of course, near the $\frac{l}{4}$ and $\frac{3l}{4}$ sections, a difference can be seen to some extent, but this effect on the total bending moment is not large. The influence line of the support bending moment is obtained

under the assumption of the effective width being 50% of the girder spacing, and thus the value itself is not always necessary to be correct. However, the point of the maximum ordinate is close to the support, compared with the case of the single continuous beam. This was pointed out first by the author and Prof. H. Yonezawa theoretically by the theory of the continuous orthotropic plate, and this experiment can explain clearly the theoretical result.

7. Results of Experiment of the Steel Deck and the Discussion

a) Stress Distribution of the Upper Surface of the Steel Deck in the Main Girder Test

1. Distribution of stress σ_x. The distribution of σ_x is shown in fig. 7. The measured value of the stress directly under the applied load can not be relied upon very much, and moreover the magnitude of the stresses are so small

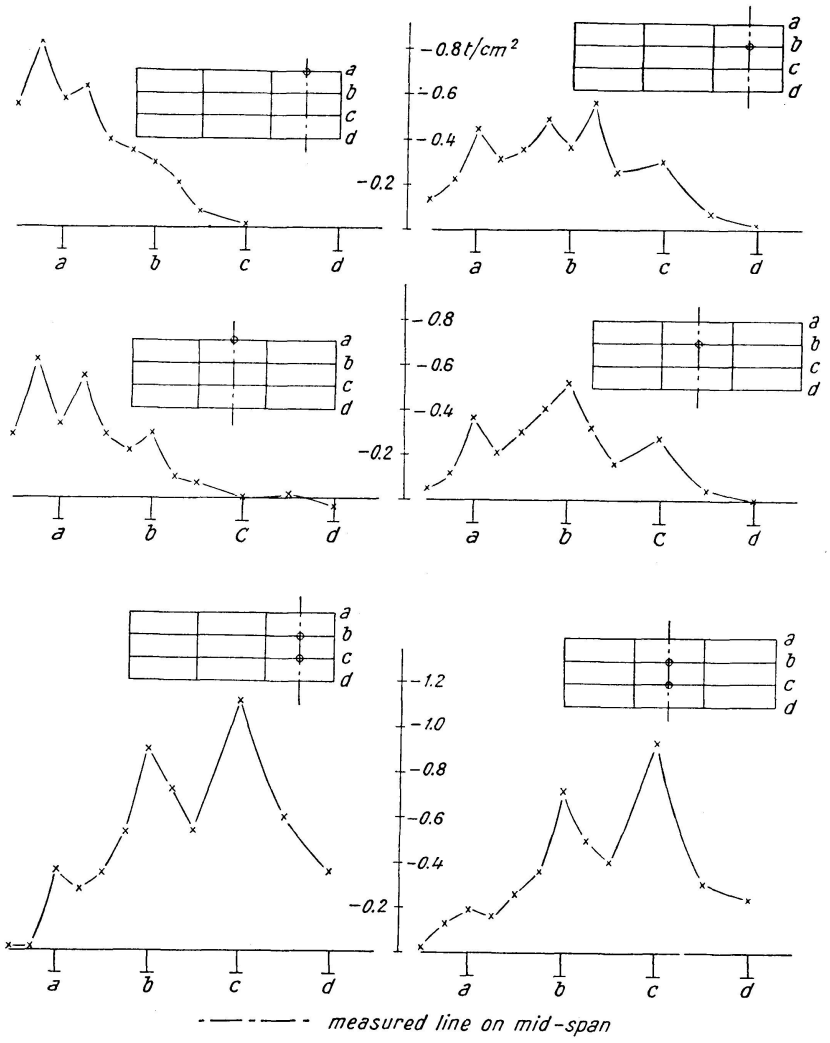

Fig. 7a. Distribution of σ_x of the Upper Surface of Deck with Sway Bracing, ° Load 30 t.

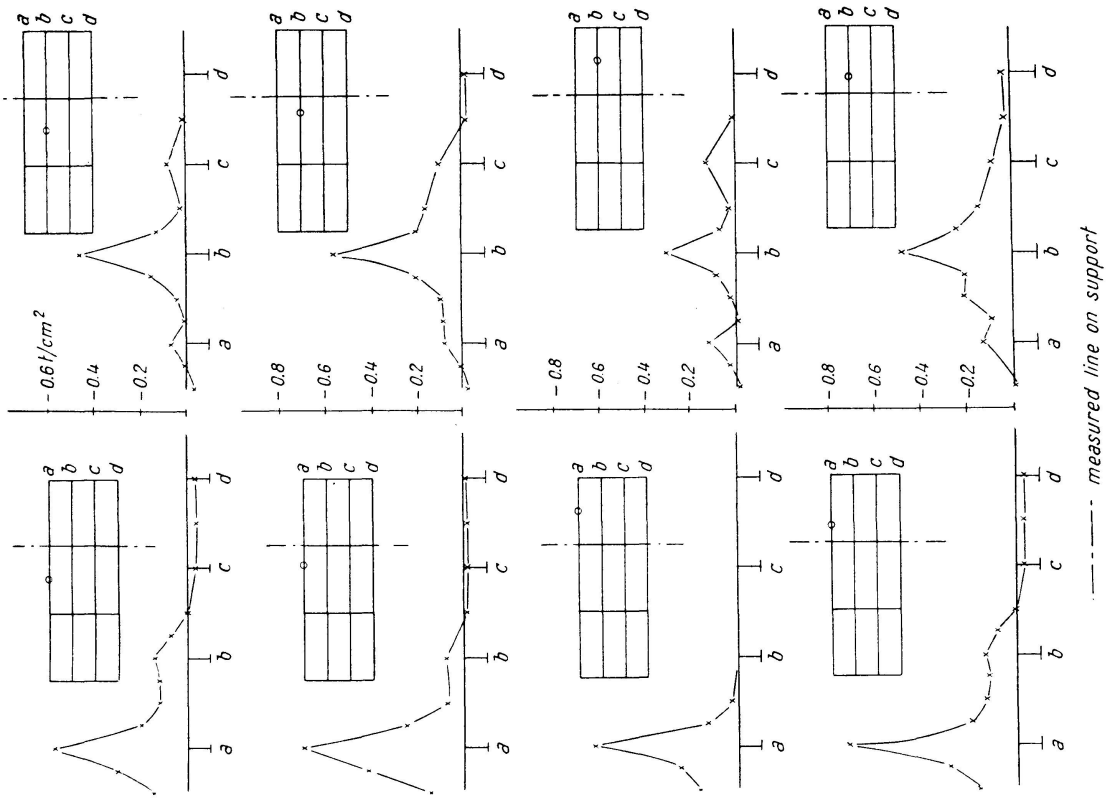

Fig. 7c. Distribution of σ_x of the Upper Surface of Deck with Sway Bracing, ° Load 30 t.

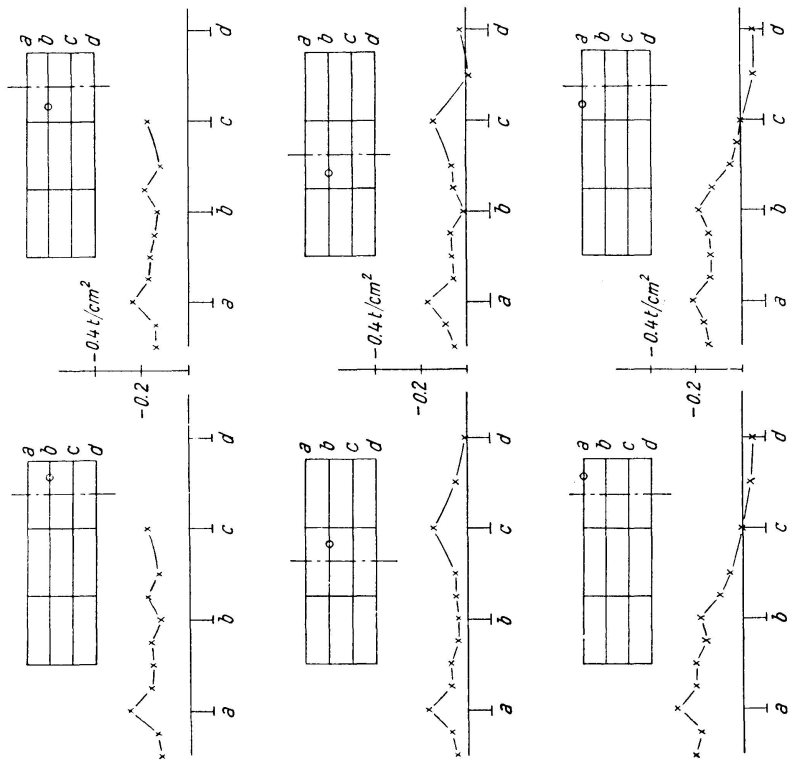

Fig. 7b. Distribution of σ_x of the Upper Surface of Deck with Sway Bracing, ° Load 30 t.

that we shall not discuss the values, but discuss the effective width of the upper flange.

a) Calculation of the effective width. According to Prof. Schade, we can calculate the effective width of the section of the maximum bending moment between the sections of zero bending moment. Because the external forces on the test girder bridge are the concentrated loads applied by hydraulic jacks and support reactions as concentrated loads and the reaction from the neighbouring main girders as a distributed load, we shall consider the effective width for both loads.

As the form of the bending moment diagram of each girder of the continuous girder structure does not differ very much from that of the single continuous girder, we shall use the bending moment diagram of the single continuous beam girder. We shall obtain the following table and figure.

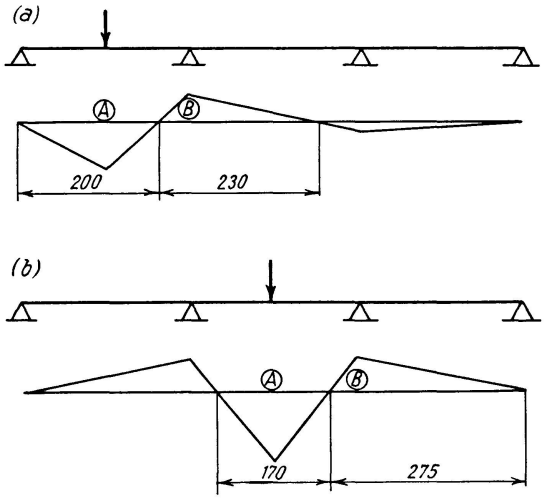

	l	l/B	effective width	
			concentrated load	distributed load
(a)	200 cm	2.5	0.60 B	0.82 B
	230 cm	2.9	0.65 B	0.90 B
(b)	170 cm	2.1	0.52 B	0.75 B
	270 cm	3.4	0.67 B	0.95 B

B = girder spacing

b) Consideration of effective width. In this experiment, the effective width of the upper flange is, as can be understood from the above calculation, $50 \sim 60\%$ of the girder spacing for the concentrated load, and $75 \sim 95\%$ for the distributed load. Near the support, the deflection of each girder does not differ greatly from each other and the reaction force from the neighbouring girders (distributed load) is small compared with the support reaction (con-

centrated load). Therefore, the effective width is almost equal to that due to concentrated load.

As the reaction from the neighbouring girders is larger near the mid-span than that near the supports, it is assumed that the effective width approaches closer to the width due to the distributed load at the mid-span than near the supports. Moreover, when the measured point does not coincide with the point where the load is applied, the influence of the concentrated load is smaller than the previous case and the effective width seems to be larger. This fact can be understood by comparing fig. 7, a, b and c.

Generally speaking, it seems proper to assume that the effective width is $50 \sim 60\%$ of the girder spacing at the supports and $80 \sim 90\%$ at the mid-span. It can be understood from fig. 8 that the latter assumption is almost correct.

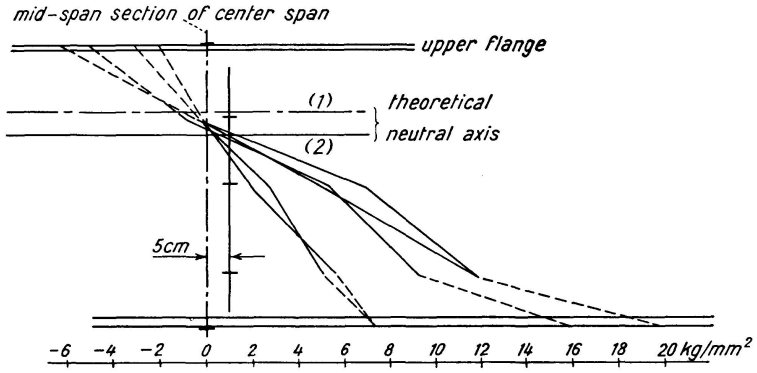

Fig. 8. Stress of Web Plate. Strain Gage: (1) Effective Width = Girder Spacing. (2) Effective Width = $\frac{2}{3}\times$ Girder Spacing.

2. Distribution of stress σ_y. The distribution of stress σ_y under the load applied to the mid-span section of the center span of the inside girder is shown in fig. 9. It is understood from this figure that the distribution is singular on the main girder. Except the neighbourhood of the load (on the longitudinal stiffener neighbouring to the main girder), the stress σ_x in the direction of the main girder is constant. Thus, we can assume that we can adopt the full width of the cross sway bracing as the effective width.

b) Stress Distribution of the Steel Deck in Deck Test

1. The case where the load is applied to the panel point (the intersecting point of transverse and longitudinal stiffeners). The stress distribution is shown in fig. 10, 11 and 12. From fig. 10, it is understood that the steel deck is supported continuously by the main girders, because the loaded transverse stiffener and the neighbouring two stiffeners produce negative bending moments on the main girder and positive bending moments near the loaded points.

Let us compare the measured values with the theoretical values. The theoretical values are calculated by the theory of the single and continuous steel deck.

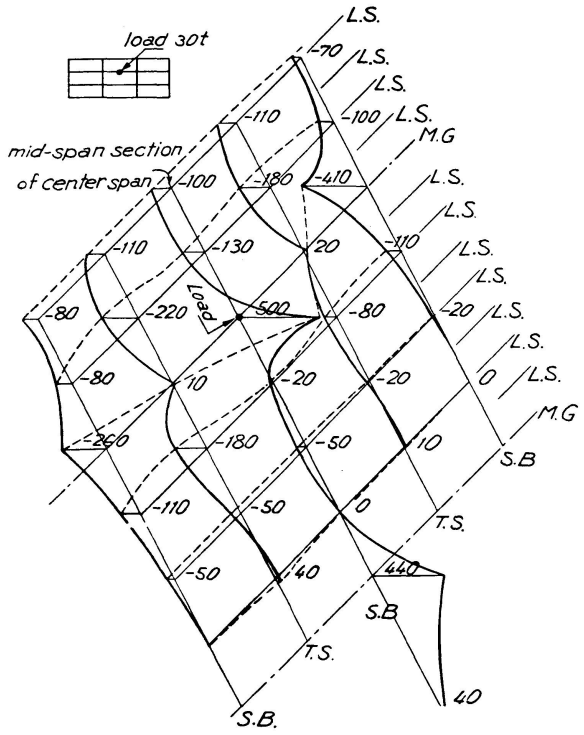

Fig. 9a. Distribution of σ_y of the Upper Surface of Deck with Sway Bracing.

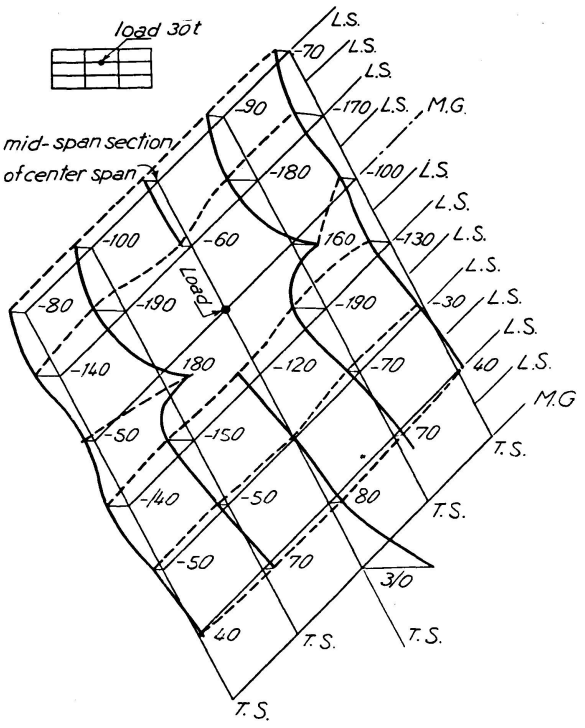

Fig. 9b. Distribution of σ_y of the Upper Surface of Deck without Sway Bracing.

T.S. Transverse Stiffener. M.G. Main Girder. L.S. Longitudinal Stiffener. S.B. Sway Bracing.

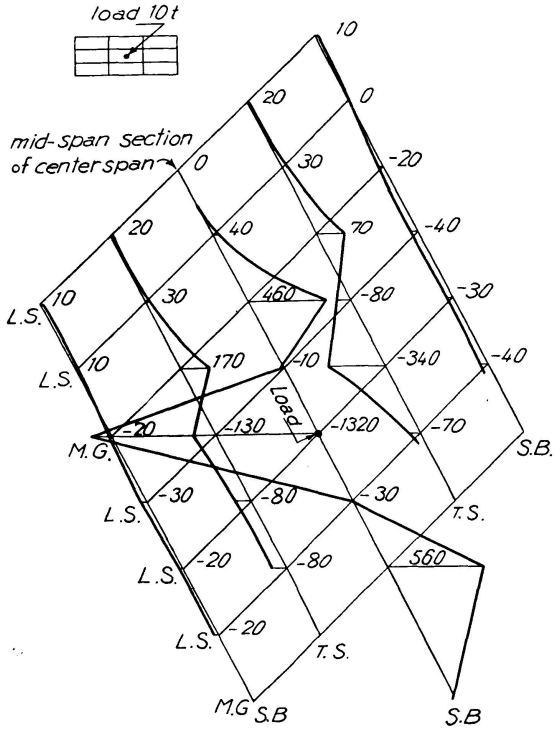

Fig. 10a. Distribution of σ_y of the Upper Surface of Deck with Sway Bracing.

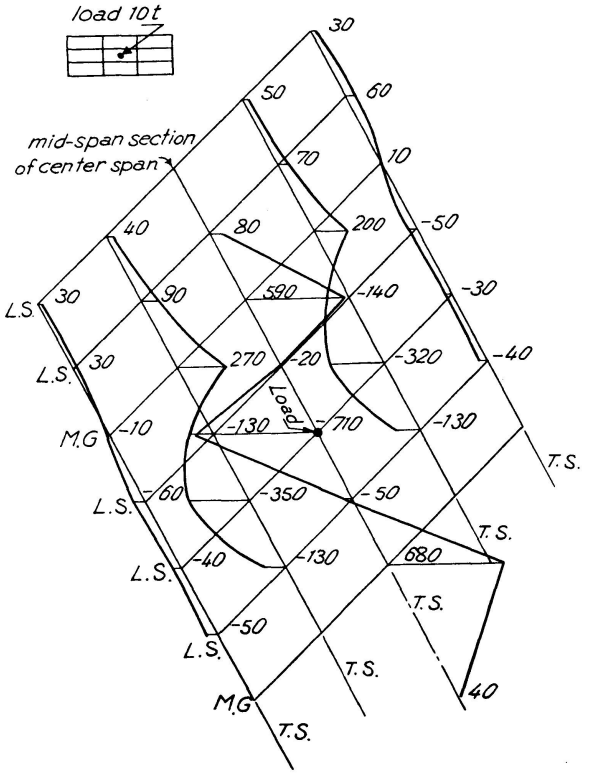

Fig. 10b. Distribution of σ_y of the Upper Surface of Deck without Sway Bracing.

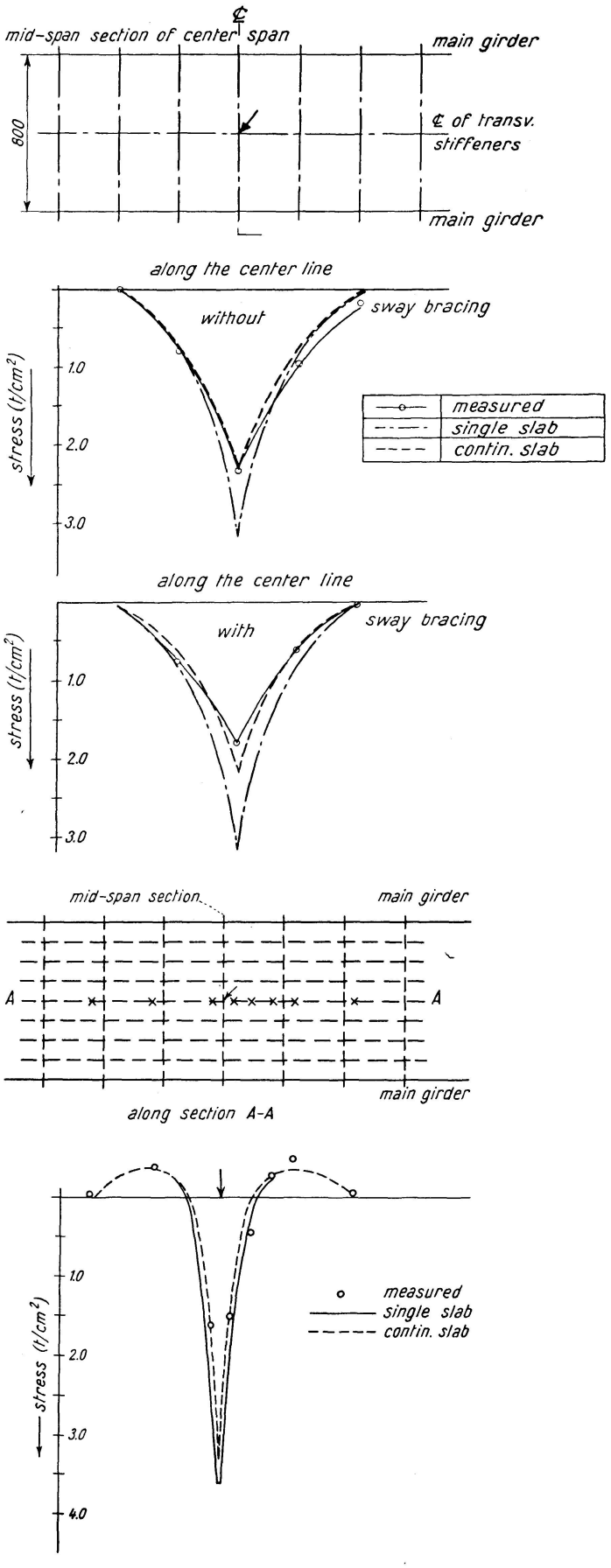

Fig. 11. Stress Distribution of Transverse Stiffeners.

Fig. 12. Stress Distribution of Longitudinal Stiffener without Sway Bracing.

The former method of calculation is based on the assumption that the deck is a plate with simply supported edges on the opposite two sides (longitudinal stiffeners) and with infinite length in its direction. We calculate the theoretical values by Cornelius's method using the following values;

$$B_y = \frac{EJ_y}{30}, \qquad B_x = \frac{EJ_x}{10}, \qquad J_y = 302.3 \text{ cm}^4, \qquad J_x = 22.8 \text{ cm}^4,$$

$$\kappa = \frac{H}{\sqrt{B_x B_y}} = 0.4.$$

The latter method is so complex that we shall use the conventional method. That is, because the flexural rigidity of the main girder is so much larger than that of the transverse stiffener that we can consider that the transverse stiffener is a three span continuous girder supported rigidly by the main girder, we use the reduced moment of inertia $J_y = 424.0$ cm^4 instead of its original value $J_y = 302.3$ cm^4, the other procedure being the same as above.

The theoretical values are plotted in fig. 11, 12. From fig. 11, the theoretical values calculated by the latter method agreed better with the measured values than the values calculated by the former method.

The comparison of the stress of the longitudinal stiffeners is shown in fig. 12. It can be said that the theoretical and measured values coincide with each other.

2. The case when the load was applied to the mid-span of the longitudinal

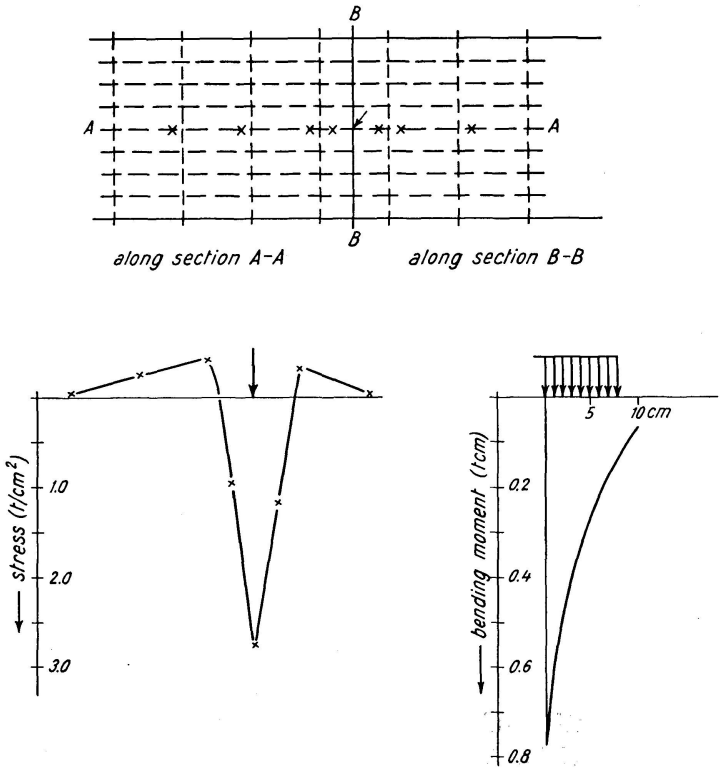

Fig. 13. Stress Distribution of Longitudinal Stiffeners without Sway Bracing.

stiffener. The stress of the longitudinal stiffener is shown in fig. 13. Two methods of calculation can be considered.

a) If we consider the steel deck as an orthotropic plate with a reduced flexural rigidity in the x-direction, with the flexural rigidity of the steel deck plate only in the y-direction and also with the simply supported boundary conditions at the opposite two edges (transverse stiffeners), the theoretical stress is 6,160 kg/cm^2. The stress ratio is $2{,}750/6{,}160 = 45\%$. The numerical values used are as follows: reduced flexural rigidity $B_x = \frac{EJ_x}{10}$, $J_x = 27.3\,\text{cm}^4$ (the longitudinal stiffeners are considered as three span continuous girders), flexural rigidity of top plate $B_y = \frac{Et^3}{12(1-\nu^2)} = 4.2 \times 10^4$ kg/cm.

b) From fig. 13, it is shown that the stringers neighbouring the loaded stringer do not share the external force. From this fact, the deck plate can be considered as a plate or membrane surrounded by transverse stiffeners and two stringers neighbouring the loaded one. According to this analysis, a considerable difference does not exist and the maximum stress is 5,800 kg/cm^2.

8. Conclusion

From the above descriptions, the followings can be concluded.

1. The measured values agree with the theoretical values for the deflection and bending moment at the mid-span. For the deflection and bending moment at the mid-span, the method using the reduced moment of inertia such as F. Leonhardt's method and the theory of orthotropic plates is sufficient. However, if these methods are applied to the calculation of the deflection and bending moment at any section except the mid-span section, an error is inevitable.

2. The sway bracing plays the roll of distributing the load to each girder to a certain extent. This action must be taken into the calculation of the load distribution. The flexural rigidity of the sway bracing can be calculated from the cases of symmetrical and skew-symmetrical loadings as shown in fig. 16. However, the above procedure is limited to the case of four girders. For the case of more than five main girders, a suitable method remains to be solved.

3. It can be surely said that the steel deck must be calculated as an orthotropic continuous plate. Some conventional methods were described above. Moreover, a further study is necessary to solve many unknown points.

References

1. Pippard, A. J. S., Studies in Elastic Structures. London 1952, p. 96.
2. Krieger, W., Ingenieur-Archiv, 17 (1949), S. 391.
3. Leonhardt, F., Die vereinfachte Trägerrostberechnung, Stuttgart 1950.
4. Homberg, H., Statik der Trägerroste und Platten, Berlin 1951.
5. Homberg, H., Stahlbau 21 (1952), S. 42, 64, 77, 100.

6. GUYON, Y., Annales des Ponts et Chaussées. Septembre, octobre 1946, p. 553, 612. MASSONNET, CH., Publication of I.A.B.S.E., 10 (1950), p. 147.
7. NARUOKA, M. and YONEZAWA, H., Proceedings of the 5th Japan National Congress for Applied Mechanics, 1955, p. 107.

Appendix A: The Flexural Rigidity of the Main Girder and Cross Girder

1. The rigidity of main girder. The spacing of girder "λ" can be considered as the effective width of the main girder for the symmetrical load, and the effective width must be chosen as $2\lambda/3$ only when the inside girders are loaded skew-symmetrically, as shown in fig. 14b, but for the other cases "λ" can be considered as the effective width.

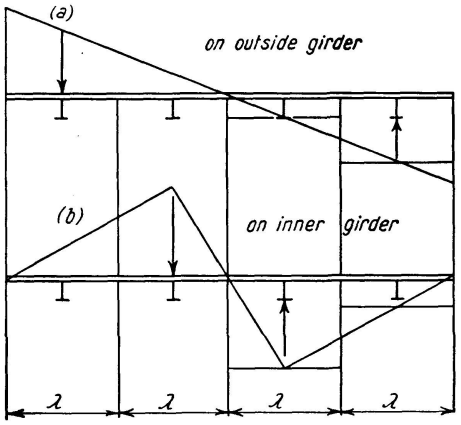

Fig. 14. Skew-Symmetrical Load.

In applying the grillage girder theory or the orthotropic plate theory to the analysis of this bridge, the converted moment of inertia of the main girder must be calculated. We considered that the existence of the deflection of the girder due to shearing forces reduces the flexural rigidity of the main girder and calculated the converted flexural rigidity, taking the shearing forces into account.

2. Rigidity of cross girder. The sway bracing plays an important part in the load distribution. This can be clearly understood by experiments. The converted flexural rigidity of the cross girder can be calculated as follows:

We consider the transverse stiffener-sway bracing system as a girder stiffened by truss members and calculate the deflection of this stiffened girder for both symmetrical and skew-symmetrical loadings (fig. 15, 16). Then assuming a girder which shows the same deflection, the converted moments of inertia are calculated for these two cases.

It must be noticed that there is a considerable difference in the converted moments of inertia of the two cases as can be understood from table 1. This is due to the fact that the deflection due to shearing force is fairly large in the stiffened truss. Therefore, the calculation in the case of single load must be done by superposing the results of the calculation for the symmetrical and

skew-symmetrical loads and the converted moment of inertia for these two cases should be used.

It is not preferable to use the converted flexural rigidity of the case when a single load is put on the stiffener-bracing system shown in fig. 16c as that for the single load, because the system receives a reaction from the main girder even when a single load is applied to one of the main girders and this case is not equal to the single load case shown in fig. 16c.

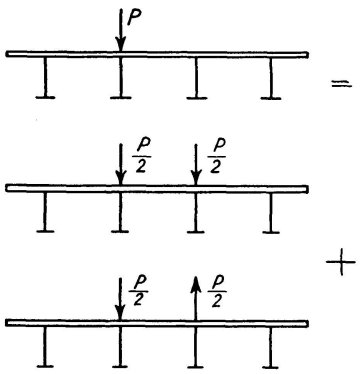

Fig. 15. Composition of Load.

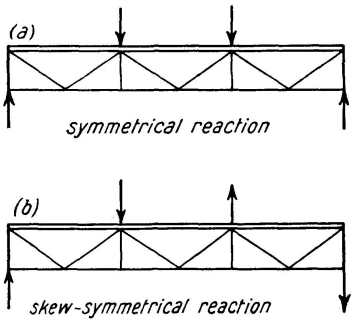

Fig. 16.

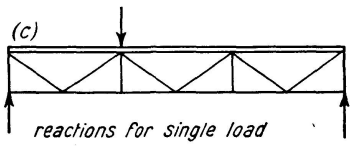

Appendix B

In this appendix, the solutions are obtained for the cases of bridges with four main girders under certain convenient assumptions. In the first place, the floor system is assumed to prevent any twisting of the main girder, and in the second place, the cross girders are replaced by a continuous connecting system which is able to resist transverse bending without increasing the longitudinal strength of the bridge.

1. Notations

l	span of the girder.
c	distance of the position of the load from the support.
a	spacing of the main girders.
J	reduced moment of inertia of cross girder per unit length.
$I_1\,(I_2)$	moments of inertia of outside (inside) main girder.
$A_1\,(A_2)$	sectional area of outside (inside) main girder.
$y_{0,m}\,(y_{0,s})$	deflections of main girder caused by bending moment (shearing force) due to concentrated load.
$y_{1,m}\,(y_{2,m}), y_{1,s}\,(y_{2,s})$	deflections of outside (inside) girder caused by bending moment (shearing force) due to symmetrical load.

$z_{1,m}(z_{2,m}), z_{1,s}(z_{2,s})$ deflections of outside (inside) girder caused by bending moment (shearing force) due to skew-symmetrical load.

$y_1=y_{1,m}+y_{1,s}$, $y_2=y_{2,m}+y_{2,s}$ deflections of outside (inside) girder due to symmetrical load.

$z_1=z_{1,m}+z_{1,s}$, $z_2=z_{2,m}+z_{2,s}$ deflections of outside (inside) girder due to skew symmetrical load.

$$y_m = y_{2,m}-y_{1,m}, \qquad y_s = y_{2,s}-y_{1,s},$$
$$z_m = \frac{z_{2,m}-z_{1,m}}{3}, \qquad z_s = \frac{z_{2,s}-z_{1,s}}{3}.$$

$\gamma=\frac{5a^3}{6EJ}$ the reciprocal of the spring constant for the case of symmetrical load.

$\gamma'=\frac{a^3}{18EJ}$ the reciprocal of the spring constant for the case of skew-symmetrical load.

κ_0 the ratio of maximum shearing stress to average shearing stress when the section is subjected to bending.

$$\beta_1=\frac{I_2}{I_1}, \quad \beta_2=\frac{I_1}{I_2}=\frac{1}{\beta_1}, \quad \beta_1'=\frac{A_2}{A_1}, \quad \beta_2'=\frac{A_1}{A_2}=\frac{1}{\beta_1'};$$
$$\mu=\frac{1+\beta_1}{EI_2\gamma}, \qquad k=\frac{1+\beta_1'}{\kappa_0 GA_2\gamma},$$
$$\mu'=\frac{9+\beta_1}{3EI_2\gamma'}, \qquad k'=\frac{9+\beta_1'}{3\kappa_0 GA_2\gamma'};$$
$$\lambda=\frac{EI_2}{\kappa_0 GA_2 l^2};$$
$$\alpha,\beta = 0.5\,[2\,(\mu)^{1/2}\pm k]^{1/2}, \qquad \eta,\delta = 0.5\,[2\,(\mu')^{1/2}\pm k']^{1/2};$$
$$b_1=\frac{2P}{EI_2 l}, \qquad b_2=\frac{2P}{\kappa_0 GA_2 l};$$

$$\varphi_1,\varphi_5(\alpha,\beta,x) = (\alpha^2-\beta^2)\exp(\ \alpha x)\cos\beta x \pm 2\alpha\beta\exp(\ \alpha x)\sin\beta x,$$
$$\varphi_2,\varphi_6(\alpha,\beta,x) = (\alpha^2-\beta^2)\exp(\ \alpha x)\sin\beta x \pm 2\alpha\beta\exp(\ \alpha x)\cos\beta x,$$
$$\varphi_3,\varphi_7(\alpha,\beta,x) = (\alpha^2-\beta^2)\exp(-\alpha x)\cos\beta x \pm 2\alpha\beta\exp(-\alpha x)\sin\beta x,$$
$$\varphi_4,\varphi_8(\alpha,\beta,x) = (\alpha^2-\beta^2)\exp(-\alpha x)\sin\beta x \pm 2\alpha\beta\exp(-\alpha x)\cos\beta x.$$

2. General Relations

a) Generally speaking, the relation between the deflection due to bending moment y_m and deflection due to shearing force y_s can be determined by the following procedure.

$$\frac{d^2y_m}{dx^2}=-\frac{M}{EI}, \qquad \frac{dy_s}{dx}=\kappa_0\frac{Q}{GA}, \qquad \frac{d^3y_m}{dx^3}=-\frac{1}{EI}\frac{dM}{dx}=-\frac{Q}{EI},$$
$$\therefore\ EI\frac{d^3y_m}{dx^3}+\kappa_0 GA\frac{dy_s}{dx}=0. \tag{a}$$

b) The value of support bending moment of the three span continuous girder with equal span and equal flexural rigidity.

For the side span loading, there is the following relation (fig. 17a);

$$M_1 = \frac{8\,M_{10}}{15}. \tag{b}$$

For the center span loading, there is the following relation (fig. 17b);

$$\begin{aligned} &M_1 = M_0 + \Delta M, \qquad M_0 = \frac{9}{15}\,\frac{M_{10}+M_{20}}{2}, \\ &M_2 = M_0 - \Delta M, \qquad \Delta M = P\,a\,b\,\frac{b-a}{15\,l^2}. \end{aligned} \tag{c}$$

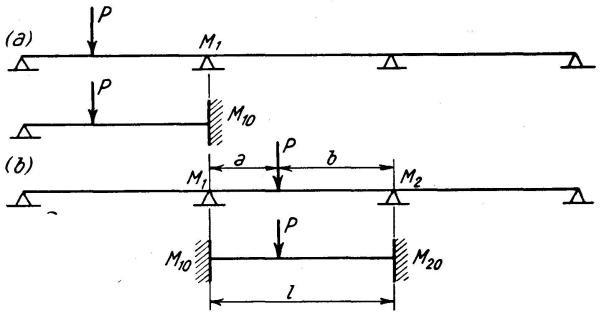

Fig. 17.

Chapter 1. Case Where the Load is Applied to the Inside Girder

A. Symmetrical Load

1. Induction of the fundamental differential equation (fig. 18). The relative deflections y_m and y_s of the outside and inside girders due to bending moment and shearing force can be expressed as follows.

$$y_m = y_{2,m} - y_{1,m}, \qquad y_s = y_{2,s} - y_{1,s}, \qquad y_1 = y_{1,m} + y_{1,s}$$

$$y_2 = y_{2,m} + y_{2,s}, \qquad y_2 - y_1 = y_m + y_s, \qquad \therefore \frac{y_m + + y_s}{\gamma} = p_1 = p_2.$$

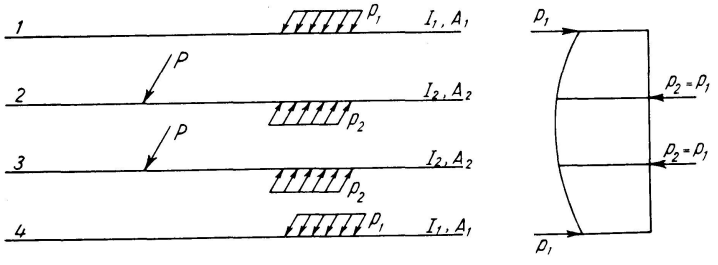

Fig. 18.

The following four differential equations are obtained for the outside and inside girders

$$EI_1\frac{d^4y_{1,m}}{dx^4}=p_1, \quad (1) \qquad EI_2\frac{d^4(y_{0,m}-y_{2,m})}{dx^4}=p_2=p_1. \quad (2)$$

$$\kappa_0 GA_1\frac{d^2y_{1,s}}{dx^2}=-p_1, \quad (3) \qquad \kappa_0 GA_2\frac{d^2(y_{0,s}-y_{2,s})}{dx^2}=-p_2=-p_1. \quad (4)$$

By subtracting eq. (2) from eq. (1) and also eq. (4) from eq. (3), the following two differential equations are obtained.

$$\frac{d^4(\beta_2 y_{1,m}+y_{2,m}-y_{0,m})}{dx^4}=0, \quad (5) \qquad \frac{d^2(\beta_2' y_{1,s}+y_{2,s}-y_{0,s})}{dx^2}=0. \quad (6)$$

Addition of eq. (1) multiplied by β_1 to eq. (2) gives

$$EI_2\frac{d^4(y_{1,m}-y_{2,m}+y_{0,m})}{dx^4}=p_1(1+\beta_1), \qquad \therefore \frac{d^4(y_m-y_{0,m})}{dx^4}=-\mu(y_m+y_s),$$

$$\therefore \frac{d^4y_m}{dx^4}+\mu y_m+\mu y_s=\frac{d^4y_{0,m}}{dx^4}. \quad (7)$$

The same procedure for eq. (3) and (4) gives

$$\frac{d^2y_s}{dx^2}-ky_s-ky_m=\frac{d^2y_{0,s}}{dx^2}. \quad (8)$$

From eq. (7), we get

$$\frac{d^2y_s}{dx^2}=-\frac{1}{\mu}\frac{d^6y_m}{dx^6}-\frac{d^2y_m}{dx^2}+\frac{1}{\mu}\frac{d^6y_{0,m}}{dx^6}. \quad (9)$$

Substituting eq. (9) into eq. (8), we obtain

$$\frac{d^6y_m}{dx^6}-k\frac{d^4y_m}{dx^4}+\mu\frac{d^2y_m}{dx^2}=\frac{d^6y_{0,m}}{dx^6}-k\frac{d^4y_{0,m}}{dx^4}-\mu\frac{d^2y_{0,s}}{dx^2}. \quad (10')$$

If we can assume $\beta_1\doteqdot\beta_1'$, the relation $k\frac{d^4y_{0,m}}{dx^4}+\mu\frac{d^2y_{0,s}}{dx^2}=0$ can be obtained. Therefore, finally the important differential equation

$$\frac{d^6y_m}{dx^6}-k\frac{d^4y_m}{dx^4}+\mu\frac{d^2y_m}{dx^2}=\frac{d^6y_{0,m}}{dx^6} \quad (10)$$

can be obtained. The term on the right side of eq. (10) is previously given for the given state of loading. Thus, the above differential equation can be solved. If $y_m=y_{2,m}-y_{1,m}$ is obtained, the term $y_s=y_{2,s}-y_{1,s}$ can also be obtained from eq. (9).

From eq. (5) and (6), the terms $\beta_2 y_{1,m}+y_{2,m}-y_{0,m}$ and $\beta_2' y_{1,s}+y_{2,s}-y_{0,s}$ are given.

Because $y_m=y_{2,m}-y_{1,m}$ and $y_s=y_{2,s}-y_{1,s}$ are previously determined, terms $y_{1,m}$, $y_{2,m}$, $y_{1,s}$ and $y_{2,s}$ can be obtained. Thus, the deflections $y_1=y_{1,m}+y_{1,s}$, $y_2=y_{2,m}+y_{2,s}$ can be determined.

2. Solution of the fundamental differential equation and deduction of deflection y_1 and y_2.

a) When the load is applied to the girder which is simply supported at the one end, and is fixed at the other end (fig. 19). The deflections $y_{0,m}$ and $y_{0,s}$ of the girder shown in fig. 18 can be expressed as follows from eq. (a).

$$\begin{aligned} y_{0,m} &= b_1 \sum \left(\frac{l}{n\pi}\right)^4 \sin\frac{n\pi c}{l}\sin\frac{n\pi x}{l} + \frac{1}{6}A_1 x^3 + \frac{1}{2}A_2 x^2 + A_3 x + A_4, \\ y_{0,s} &= b_2 \sum \left(\frac{l}{n\pi}\right)^2 \sin\frac{n\pi c}{l}\sin\frac{n\pi x}{l} - \lambda l^2 A_1 x + A_0. \end{aligned} \tag{11}$$

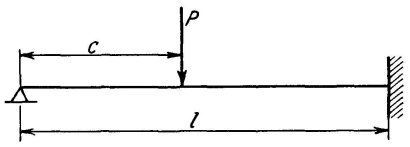

Fig. 19.

The boundary conditions are as follows.

at $x = 0$: $\quad y_{0,m} + y_{0,s} = 0, \quad \dfrac{d^2 y_{0,m}}{dx^2} = 0,$

at $x = l$: $\quad y_{0,m} + y_{0,s} = 0, \quad \dfrac{dy_{0,m}}{dx} = 0.$

Substitution of above eq. into eq. (11) gives the integral constants as follows:

$$\begin{aligned} A_0 &= A_2 = A_4 = 0, \\ A_1 &= -\frac{2P}{\pi^3 E I_2}\sum \frac{\frac{(-1)^n}{n^3}\sin\frac{n\pi c}{l}}{\frac{1}{3}+\lambda}, \\ A_3 &= \frac{2Pl^2}{\pi^3 E I_2}\sum \frac{\left(\frac{1}{6}-\lambda\right)\frac{(-1)^n}{n^3}\sin\frac{n\pi c}{l}}{\frac{1}{3}+\lambda}. \end{aligned} \tag{12}$$

Substituting eq. (11) into eq. (10), we obtain

$$\frac{d^6 y_m}{dx^6} - k\frac{d^4 y_m}{dx^4} + \mu\frac{d^2 y_m}{dx^2} = -\frac{2P}{E I_2 l}\sum \left(\frac{n\pi}{l}\right)^2 \sin\frac{n\pi c}{l}\sin\frac{n\pi x}{l}. \tag{13}$$

Solution of the above differential equation is as follows:

$$\begin{aligned} y_m = {} & \frac{1}{\alpha^2+\beta^2}\left[B_1\varphi_5(\alpha,\beta,x) + B_2\varphi_6(\alpha,\beta,x) + B_3\varphi_7(\alpha,\beta,x) + B_4\varphi_8(\alpha,\beta,x)\right] \\ & + B_5 x + B_6 + \frac{2P}{E I_2 l}\sum \frac{\sin\frac{n\pi c}{l}\sin\frac{n\pi x}{l}}{\left(\frac{n\pi}{l}\right)^4 + k\left(\frac{n\pi}{l}\right)^2 + \mu}. \end{aligned} \tag{14}$$

From eq. (7), the relative deflection can be obtained as follows:

$$y = y_m + y_s = -\frac{1}{\mu}\frac{d^4 y_m}{dx^4} + \frac{1}{\mu}\frac{d^4 y_{0,m}}{dx^4}.$$

Therefore, the use of eq. (14) gives the following

$$\begin{aligned} y = &-\frac{1}{\mu}[B_1\varphi_1(\alpha,\beta,x) + B_2\varphi_2(\alpha,\beta,x) + B_3\varphi_3(\alpha,\beta,x) + B_4\varphi_4(\alpha,\beta,x)] \\ &+ \frac{b_1}{\mu}\frac{k\left(\frac{l}{n\pi}\right) + \mu\left(\frac{l}{n\pi}\right)^3}{\left(\frac{n\pi}{l}\right) + k\left(\frac{l}{n\pi}\right) + \mu\left(\frac{l}{n\pi}\right)^3}\sin\frac{n\pi c}{l}\sin\frac{n\pi x}{l}. \end{aligned} \tag{15}$$

From the boundary conditions at $x=0$, $y=0$, $\frac{d^2 y_m}{dx^2}=0$ and at $x=l$, $y=0$, $\frac{dy_m}{dx}=0$, the integral constants can be determined as follows.

$$\begin{aligned} &B_1 = -B_3 = -\frac{D_1 \Delta_4}{\Delta_1\Delta_4 - \Delta_2\Delta_3}, \quad B_2 = B_4 = \frac{D_1\Delta_3}{\Delta_1\Delta_4 - \Delta_2\Delta_3}, \\ &\Delta_1 = 2R + 2(\ U\cosh\alpha l\cos\beta l + W\sinh l\sin\beta l)\kappa_0 G A_2, \\ &\Delta_2 = 2S + 2(-W\cosh\alpha l\cos\beta l + U\sinh\alpha l\sin\beta l)\kappa_0 G A_2, \\ &\Delta_3 = 2(\alpha^2-\beta^2)\sinh\alpha l\cos\beta l - 4\alpha\beta\cosh\alpha l\sin\beta l, \\ &\Delta_4 = 2(\alpha^2-\beta^2)\cosh\alpha l\sin\beta l + 4\alpha\beta\sinh\alpha l\cos\beta l, \\ &R = EI_2\alpha - \kappa_0 G A_2\left(U + \frac{K_4}{\mu}\right), \quad S = EI_2\beta - \kappa_0 G A_2\left(-W + \frac{K_5}{\mu}\right), \\ &U = \frac{K_1}{K_3}, \quad W = \frac{K_2}{K_3}, \\ &K_1 = \alpha(\alpha^2+\beta^2), \quad K_2 = \beta(\alpha^2+\beta^2), \quad K_3 = (\alpha^2+\beta^2)^2, \\ &K_4 = \alpha(\alpha^2-3\beta^2), \quad K_5 = \beta(3\alpha^2-\beta^2), \\ &D_1 = b_1\sum\frac{\left\{\kappa_0 G A_2\left[\left(\frac{l}{n\pi}\right)^2(-1)^n + \frac{k}{\mu}\right] - EI_2\right\}}{\left(\frac{n\pi}{l}\right) + k\left(\frac{l}{n\pi}\right) + \mu\left(\frac{l}{n\pi}\right)^3}\sin\frac{n\pi c}{l}. \end{aligned} \tag{16}$$

b) When the load is applied to the side span of the three span continuous girder with equal span and equal flexural rigidity (fig. 17 a).

The ratio of support bending moment (M_1) of the three span continuous girder to that (M_{10}) of the girder with the simply supported and fixed end is $\frac{M_1}{M_{10}} \fallingdotseq \frac{8}{15}$. Thus, the integral constants determined in a) can be applied to the side span of the continuous girder by multiplying the factor $\frac{8}{15}$. Therefore, if we adopt the integral constants which are $\frac{8}{15}$ times as large as that of eq. (16), the equations of deflection (11) and (15) can be applied to this case with no modification.

Rewriting the eq. (5) and (6), we have

$$\frac{d^4(\beta_2 y_{1,m}+y_{2,m}-y_{0,m})}{dx^4}=0, \qquad \frac{d^2(\beta_2' y_{1,s}+y_{2,s}-y_{0,s})}{dx^2}=0.$$

For the case of this girder the above two equations become zero, namely

$$\beta_2 y_{1,m}+y_{2,m}-y_{0,m}=0, \qquad \beta_2' y_{1,s}+y_{2,s}-y_{0,s}=0.$$

Addition of the above two equations under the assumption $\beta_2=\beta_2'$ gives,

$$\beta_2(y_{1,m}+y_{1,s})+(y_{2,m}+y_{2,s})-(y_{0,m}+y_{0,s})=\beta_2 y_1+y_2-y_0=0.$$

The relative deflection can be written as follows:

$$y=y_m+y_s=(y_{2,m}-y_{1,m})+(y_{2,s}-y_{1,s})=y_2-y_1.$$

Because $y_{0,m}$, $y_{0,s}$, y are given by eqs. (11) and (15), we can determine the deflections y_1 and y_2.

c) When the girder is fixed at both ends (fig. 20). The deflection $y_{0,m}$, $y_{0,s}$ of the girder shown in fig. 20 can be expressed by the same equation as eq. (11), except the last term of the right hand of $y_{0,s}$ (see eq. (11')).

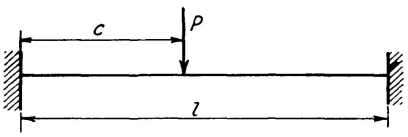

Fig. 20.

By the boundary conditions at $x=0$ and $x=l$: $y_{0,m}+y_{0,s}=0$, $\frac{dy_{0,m}}{dx}=0$, the integral constants can be determined as follows:

$$\begin{aligned}
A_1&=-\frac{P}{\pi^3 E I_2}\sum\frac{[1+(-1)^n]}{\frac{1}{12}+\lambda}\frac{1}{n^3}\sin\frac{n\pi c}{l},\\
A_2&=-\frac{2Pl}{\pi^3 E I_2}\sum\left[[-1+(-1)^n]-\frac{1+(-1)^n}{4\left(\frac{1}{12}+\lambda\right)}\right]\frac{1}{n^3}\sin\frac{n\pi c}{l},\\
A_3&=-\frac{2Pl^2}{\pi^3 E I_2}\sum\frac{1}{n^3}\sin\frac{n\pi c}{l},\\
A_4&=-\frac{2Pl^3}{\pi^3 \kappa_0 G A_2}\sum\left[[-1+(-1)^n]-\frac{1+(-1)^n}{4\left(\frac{1}{12}+\lambda\right)}\right]\frac{1}{n^3}\sin\frac{n\pi c}{l}.
\end{aligned} \tag{17}$$

The solution of fundamental eq. (10) is quite the same as eq. (15), because the term $\frac{d^6 y_{0,m}}{dx^6}$ is identical to the right side of eq. (13).

The boundary conditions at $x=0$ and $x=l$: $y=0$ and $\frac{dy_m}{dx}=0$ determine the four integral constants of eq. (15) as follows:

$$B_1=\frac{X_0}{u_0},\quad B_2=\frac{Y_0}{u_0},\quad B_3=-\frac{d_1X_0+e_1Y_0}{u_0f_1},\quad B_4=\frac{mX_0+nY_0-\frac{m}{f_1}(d_1X_0+e_1Y_0)}{u_0n},$$

where, $X_0=Ke_5+K'e_4$, $Y_0=Kd_5-K'd_4$, $u_0=d_4e_5+d_5e_4$,

$$m=\alpha^2-\beta^2,\quad n=2\alpha\beta,$$

$$K_1=\alpha(\alpha^2+\beta^2),\quad K_2=\beta(\alpha^2+\beta^2),\quad K_3=(\alpha^2+\beta^2)^2,\quad K_4=\alpha(\alpha^2-3\beta^2),$$

$$K_5=\beta(3\alpha^2-\beta^2),\quad U=K_1/K_3,\quad W=K_2/K_3,$$

$$R=EI_2\alpha-\kappa_0GA_2\left(U+\frac{K_4}{\mu}\right),\quad S=EI_2\beta-\kappa_0GA_2\left(-W+\frac{K_5}{\mu}\right),$$

$$\begin{aligned}
g_1&=U-\exp(\alpha l)(U\cos\beta l+W\sin\beta l),\ g_2=U+\exp(-\alpha l)(-U\cos\beta l+W\sin\beta l),\\
h_1&=W+\exp(\alpha l)(U\sin\beta l-W\cos\beta l),\ h_2=W-\exp(-\alpha l)(U\sin\beta l+W\cos\beta l),\\
i_1&=R+\kappa_0GA_2\exp(\ \alpha l)(U\cos\beta l+W\sin\beta l),\\
i_2&=R-\kappa_0GA_2\exp(-\alpha l)(W\sin\beta l-U\cos\beta l),\\
j_1&=S+\kappa_0GA_2\exp(\ \alpha l)(U\sin\beta l-W\cos\beta l),\\
j_2&=S-\kappa_0GA_2\exp(-\alpha l)(U\sin\beta l+W\cos\beta l),\qquad (18)\\
d_1&=m\exp(-\alpha l)(m\sin\beta l-n\cos\beta l)+n\exp(\alpha l)(m\cos\beta l-n\sin\beta l),\\
e_1&=n\exp(-\alpha l)(m\sin\beta l-n\cos\beta l)+n\exp(\alpha l)(m\sin\beta l+n\cos\beta l),\\
f_1&=m\exp(-\alpha l)(m\sin\beta l-n\cos\beta l)+n\exp(\alpha l)(m\cos\beta l+n\sin\beta l),\\
d_2&=g_1n-h_2m,\quad d_3=g_1j_1+h_2i_1,\quad d_4=f_2d_1+f_1d_2,\quad d_5=f_3d_2-f_2d_3,\\
e_2&=n(h_1+h_2),\quad e_3=j_1h_2-j_2h_1,\quad e_4=e_1f_2-e_2f_1,\quad e_5=e_2f_3+e_3f_2,\\
f_2&=g_2n+h_2m,\quad f_3=g_2j_2+h_2i_2,\\
K&=Mnf_1,\qquad K'=Mnf_3-Mj_2f_2+Lh_2f_2,
\end{aligned}$$

$$L=b_1\sum\frac{\left\{\kappa_0GA_2\left[(-1)^n\left(\frac{l}{n\pi}\right)^2+\frac{k}{\mu}\right]-EI_2\right\}}{\left(\frac{n\pi}{l}\right)+k\left(\frac{l}{n\pi}\right)+\mu\left(\frac{l}{n\pi}\right)^3}\sin\frac{n\pi c}{l},$$

$$M=b_1\sum\frac{[(-1)^n-1]\left(\frac{l}{n\pi}\right)^2}{\left(\frac{n\pi}{l}\right)+k\left(\frac{l}{n\pi}\right)+\mu\left(\frac{l}{n\pi}\right)^3}\sin\frac{n\pi c}{l}.$$

d) When the load is applied to the center span of the three span continuous girder with equal span and flexural rigidity (fig. 17 b).

The ratio of the sum of the support bending moments (M_1+M_2) of the three span continuous girder to that $(M_{10}+M_{20})$ of the girder fixed at both ends, refering to fig. 17 b, is as follows; $\frac{M_1+M_2}{M_{10}+M_{20}}\fallingdotseq\frac{9}{15}$.

Therefore, the integral constants determined in c) can be applied to the center span of the continuous girder by multiplying the factor $\frac{9}{15}$.

Thus, if we adopt the integral constants which are $\frac{9}{15}$ times as large as the integral constants of eq. (17) and (18), the equations of the deflection of the

center span of the three span continuous girder can be decided by eq. (11′) and (15′), that is,

$$y_{0,m} = b_1 \sum \left(\frac{l}{n\pi}\right)^4 \sin\frac{n\pi c}{l}\sin\frac{n\pi x}{l} + \frac{1}{6}A_1 x^3 + \frac{1}{2}A_2 x^2 + A_3 x + A_4,$$
$$y_{0,s} = b_2 \sum \left(\frac{l}{n\pi}\right)^2 \sin\frac{n\pi c}{l}\sin\frac{n\pi x}{l} - \lambda l^2 A_1 x - \lambda l^2 A_2, \tag{11′}$$

$$y = -\frac{1}{\mu}[B_1\varphi_1(\alpha,\beta,x) + B_2\varphi_2(\alpha,\beta,x) + B_3\varphi_3(\alpha,\beta,x) + B_4\varphi_4(\alpha,\beta,x)]$$
$$+ \frac{b_1}{\mu}\sum \frac{k\frac{l}{n\pi} + \mu\left(\frac{l}{n\pi}\right)^3}{\left(\frac{n\pi}{l}\right) + k\left(\frac{l}{n\pi}\right) + \mu\left(\frac{l}{n\pi}\right)^3}\sin\frac{n\pi c}{l}\sin\frac{n\pi x}{l}. \tag{15′}$$

The values of equations $\beta_2 y_{1,m} + y_{2,m} - y_{0,m}$ and $\beta_2' y_{1,s} + y_{2,s} - y_{0,s}$ are zero for this case and the values of y_1 and y_2 can be obtained by the equations $y = y_2 - y_1$ [eq. (15′) and (18)], $y_0 = \beta_2 y_1 + y_2$ [eq. (11′) and (17)].

B. Skew-Symmetrical Load

1. Induction of the fundamental differential equation refering to fig. 21. The following differential equations are obtained for the outside and inside girders by quite the same procedure.

$$z_m + z_s = \gamma' q_1,$$

$$EI_1\frac{d^4 z_{1,m}}{dx^4} = q_1, \tag{21}$$

$$EI_2\frac{d^4(y_{0,m} - z_{2,m})}{dx^4} = q_2 = 3q_1, \tag{22}$$

$$\kappa_0 G A_1\frac{d^2 z_{1,s}}{dx^2} = -q_1, \tag{23}$$

$$\kappa_0 G A_2\frac{d^2(y_{0,s} - z_{2,s})}{dx^2} = -q_2 = -3q_1, \tag{24}$$

$$\frac{d^4(3\beta_2 z_{1,m} + z_{2,m} - y_{0,m})}{dx^4} = 0, \tag{25}$$

$$\frac{d^2(3\beta_2' z_{1,s} + z_{2,s} - y_{0,s})}{dx^2} = 0, \tag{26}$$

$$\frac{d^4 z_m}{dx^4} + \mu' z_m + \mu' z_s = \frac{d^4 y_{0,m}}{dx^4}, \qquad \mu' = \frac{3 + \frac{\beta_1}{3}}{EI_2\gamma}, \tag{27}$$

$$\frac{d^2 z_s}{dx^2} - k' z_s - k' z_m = \frac{d^2 y_{0,s}}{dx^2}, \qquad k' = \frac{3 + \frac{\beta_1'}{3}}{\kappa_0 G A_2 \gamma}, \tag{28}$$

$$z_s = -\frac{1}{\mu'}\frac{d^4 z_m}{dx^4} - z_m - \frac{1}{\mu}\frac{d^4 y_{0,m}}{dx^4}, \qquad \frac{d^2 z_s}{dx^2} = -\frac{1}{\mu}\frac{d^6 z_m}{dx^6} - \frac{d^2 z_m}{dx^2} - \frac{1}{\mu}\frac{d^6 y_{0,m}}{dx^6}, \tag{29}$$

$$\frac{d^6 z_m}{dx^6} - k'\frac{d^4 z_m}{dx^4} + \mu'\frac{d^2 z_m}{dx^2} = \frac{d^6 y_{0,m}}{dx^6} - \mu'\frac{d^2 y_{0,s}}{dx^2} - k'\frac{d^4 y_{0,m}}{dx^4}, \tag{30′}$$

$$\frac{d^6 z_m}{dx^6} - k' \frac{d^4 z_m}{dx^4} + \mu' \frac{d^2 z_m}{dx^2} = \frac{d^6 y_{0,m}}{dx^6}, \tag{30}$$

if $\mu' \dfrac{d^2 y_{0,s}}{dx^2} + k' \dfrac{d^4 y_{0,m}}{dx^4} = 0$ can be assumed.

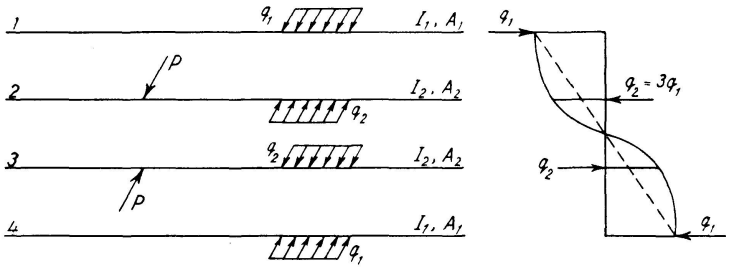

Fig. 21.

Solution of eq. (30) finally gives the value of $z_m = z_{2,m} - (1/3) z_{1,m}$.

2. Solution of the fundamental differential equation and deduction of deflections z_1 and z_2.

As for the solution of the fundamental equation when the load is applied skew-symmetrically to the inside girder, the essential parts will be described omitting the details.

a) When the girder is simply supported at the one end and is fixed at the other end. The deflection can be written as follows, refering to 1. a):

$$\begin{aligned}
y_{0,m} &= b_1 \sum \left(\frac{l}{n\pi}\right)^4 \sin\frac{n\pi c}{l} \sin\frac{n\pi x}{l} + \frac{1}{6} A_1 x^3 + A_3 x, \\
y_{0,s} &= b_2 \sum \left(\frac{l}{n\pi}\right)^2 \sin\frac{n\pi c}{l} \sin\frac{n\pi x}{l} - \lambda l^2 A_1 x, \\
z &= -\frac{1}{\mu'} [C_1 \varphi_1(\eta, \delta, x) + C_2 \varphi_2(\eta, \delta, x) + C_3(\eta, \delta, x) + C_4(\eta, \delta, x)] \\
&\quad + \frac{b_1}{\mu'} \sum \frac{k' \dfrac{l}{n\pi} + \mu' \left(\dfrac{l}{n\pi}\right)^3}{\left(\dfrac{n\pi}{l}\right) + k' \left(\dfrac{l}{n\pi}\right) + \mu' \left(\dfrac{l}{n\pi}\right)^3} \sin\frac{n\pi c}{l} \sin\frac{n\pi x}{l}.
\end{aligned} \tag{31}$$

The integral constants of the above solution z can be obtained from eq. (16) by changing the variables such as $\alpha \to \eta$, $\beta \to \delta$, $k \to k'$, $\mu \to \mu'$, and those of equation $y_{0,m}$ and $y_{0,s}$ are the same as eq. (12).

b) When the load is applied to the side span of the three span continuous girder with equal span and flexural rigidity.

From the same reason as described before, if the integral constants of eq. (31) are multiplied by factor $\frac{8}{15}$, they will be useful to the side span of the continuous girder.

For this case, $3\beta_2 z_{1,m}+z_{2,m}-y_{0,m}=0$, $3\beta_2' z_{1,s}+z_{2,s}-y_{0,s}=0$ can be obtained from eq. (25) and (26).

Therefore, $3\beta_2'' z_1+z_2-y_{0,m}-y_{0,s}=0$ can be obtained under the asumption $\beta_2''=\frac{\beta_2+\beta_2'}{2}$. On the other hand, $z=z_2-\frac{z_1}{3}$ is given by eq. (31).

Thus, we finally obtain the values of z_1 and z_2.

c) When the girder is fixed at both ends. The deflection can be written as follows, refering to 1. c):

$$
\begin{aligned}
y_{0,m} &= b_1 \sum \left(\frac{l}{n\pi}\right)^4 \sin\frac{n\pi c}{l}\sin\frac{n\pi x}{l}+\frac{1}{6}A_1x^3+\frac{1}{2}A_2x^2+A_3x+A_4,\\
y_{0,s} &= b_2 \sum \left(\frac{l}{n\pi}\right)^2 \sin\frac{n\pi c}{l}\sin\frac{n\pi x}{l}-\lambda l^2 A_1 x-\lambda l^2 A_2,
\end{aligned}
\tag{32}
$$

$$
\begin{aligned}
z = &-\frac{1}{\mu'}[C_1\varphi_1(\eta,\delta,x)+C_2\varphi_2(\eta,\delta,x)+C_3\varphi_3(\eta,\delta,x)+C_4\varphi_4(\eta,\delta,x)]\\
&+\frac{b_1}{\mu'}\sum \frac{k'\frac{l}{n\pi}+\mu'\left(\frac{l}{n\pi}\right)^3}{\left(\frac{n\pi}{l}\right)+k'\left(\frac{l}{n\pi}\right)+\mu'\left(\frac{l}{n\pi}\right)^3}\sin\frac{n\pi c}{l}\sin\frac{n\pi x}{l}.
\end{aligned}
$$

The integral constants in expressions for $y_{0,m}$ and $y_{0,s}$ are the same as those of eq. (17) and those of eq. z can be obtained by doing the same exchange of variables contained in eq. (18); that is, $\alpha\to\eta$, $\beta\to\delta$, $k\to k'$, $\mu\to\mu'$.

d) Article 4. When the load is applied to the center span of the three span continuous girder.

The equation of the deflection is useful if the integral constants described in 2. c) are multiplied by the factor $\frac{9}{15}$. The values z_1 and z_2 can be obtained from equations $3\beta_2'' z_1+z_2=y_{0,m}+y_{0,s}$, $z_2-\frac{z_1}{3}=z$ as described in 2. b).

Chapter 2. Case Where the Load is Applied to the Outside Girder

1. Symmetrical Load

Refering to fig. 22, we can obtain the following four differential equations:

$$EI_2\frac{d^4(y_{0,m}-y_{1,m})}{dx^4}=\beta_1 p_2, \tag{33}$$

$$EI_2\frac{d^4 y_{2,m}}{dx^4}=p_2, \tag{34}$$

$$\kappa_0 GA_2\frac{d^2(y_{0,s}-y_{1,s})}{dx^2}=-\beta_1' p_1=-\beta_1' p_2, \tag{35}$$

$$\kappa_0 GA_2\frac{d^2 y_{2,s}}{dx^2}=-p_2, \tag{36}$$

The same procedure as described in the above two articles finally gives the following differential equations:

$$\frac{d^4 y_m}{dx^4} + \mu y_m + \mu y_s = \frac{d^4 y_{0,m}}{dx^4}, \qquad (37) \qquad \frac{d^2 y_s}{dx^2} - k y_s - k y_m = \frac{d^2 y_{0,s}}{dx^2}, \qquad (38)$$

$$\frac{d^6 y_m}{dx^6} - k\frac{d^4 y_m}{dx^4} + \mu\frac{d^2 y_m}{dx^2} = \frac{d^6 y_{0,m}}{dx^6}. \qquad (39)$$

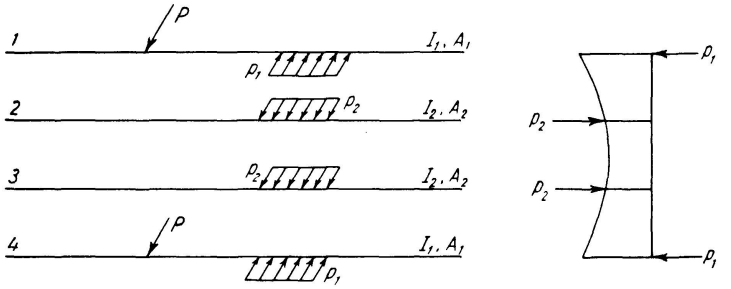

Fig. 22.

Solving the above equations, the deflection y_m, $y = y_m + y_s$ can be determined in the same way as in the previous articles. On the other hand, from $\beta_2 y_{2,m} + y_{1,m} - y_{0,m} = 0$ and $\beta' y_{2,s} + y_{1,s} - y_{0,s} = 0$ we obtain $\beta_1 y_2 + y_1 = y_{0,m} + y_{0,s}$.

From this equation and $y = y_1 - y_2$ induced above, we can obtain the values of y_1 and y_2.

2. Skew-Symmetrical Load (fig. 23)

The four differential equations corresponding to eq. (21)~(24) are as follows:

$$E I_2 \frac{d^4 (y_{0,m} - z_{1,m})}{dx^4} = \beta_1 q_1 = \frac{\beta_1 q_2}{3}, \qquad (40) \qquad E I_2 \frac{d^4 z_{2,m}}{dx^4} = q_2, \qquad (41)$$

$$\kappa_0 G A_2 \frac{d^2 (y_{0,s} - z_{1,s})}{dx^2} = -\beta_1' q_1 = -\frac{\beta_1' q_2}{3}, \qquad (42) \qquad \kappa_0 G A_2 \frac{d^2 z_{2,s}}{dx^2} = -q_2. \qquad (43)$$

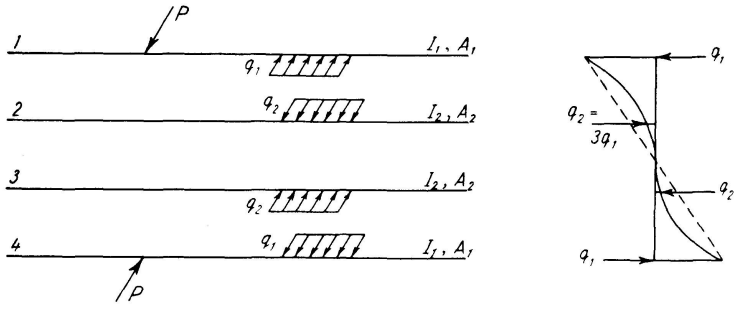

Fig. 23.

The equations corresponding to eq. (27)~(30) are

$$\frac{d^4 z_m}{dx^4} + \mu' z_m + \mu' z_s = \frac{d^4 \frac{y_{0,m}}{3}}{dx^4}, \quad (44) \qquad \frac{d^2 z_s}{dx^2} - k' z_s - k' z_m = \frac{d^2 \frac{y_{0,s}}{3}}{dx^2}, \quad (45)$$

$$\frac{d^6 z_m}{dx^6} - k' \frac{d^4 z_m}{dx^4} + \mu' \frac{d^2 z_m}{dx^2} = \frac{d^6 \frac{y_{0,m}}{3}}{dx^6}. \quad (46)$$

Solving the above equations, we finally obtain z_m and the procedure thereafter is the same as above.

The deflections y_1, y_2, z_1 and z_2 can be obtained by the same procedure as described in chapter 1 and will be omitted.

Bending Moment

From the deflections described above, we can determine the bending moment of each girder. The formula will be omitted.

Summary

An experimental study of the model of a continuous beam bridge with steel deck was made in order to clarify the problem involved in the design of a bridge such as the Kurpfalz Bridge. The stresses and deflections measured were compared with the theoretical values calculated by various methods. The authors proposed a new method which takes into account the effects of shearing force. The measured values of the deflections and stresses in main girders can be explained by any of the solutions that have been proposed, but there remain many points to be cleared up concerning stresses in the steel deck.

Résumé

Ces recherches ont été effectuées à titre de contribution à l'établissement d'un projet de pont analogue au Pont de Kurpfalz.

Les contraintes et déformations mesurées ont été comparées avec les valeurs théoriques, obtenues par application de différentes méthodes de calcul. Les auteurs proposent une nouvelle méthode qui tient compte des contraintes de cisaillement.

Les valeurs mesurées des déformations et des contraintes dans les poutres principales peuvent être expliquées par toutes les solutions proposées; il reste toutefois de nombreux points non élucidés concernant les contraintes dans le tablier métallique.

Zusammenfassung

Diese Untersuchung am Modell einer Durchlaufträgerbrücke mit Stahlfahrbahn wurde durchgeführt um einen Beitrag zur Projektierung einer Brücke analog der Kurpfalz-Brücke zu leisten.

Die gemessenen Spannungen und Deformationen wurden mit den theoretischen Werten verglichen, die aus verschiedenen Rechnungsmethoden hervorgegangen sind. Die Autoren schlagen eine neue Methode vor, die die Schubspannungen berücksichtigt.

Die gemessenen Werte der Durchbiegungen und Spannungen in den Hauptträgern können durch alle vorgeschlagenen Lösungen erklärt werden, aber es bleiben viele ungeklärte Punkte über die Spannungen in der Stahlfahrbahn zu lösen.